0026-895X/93/020336-10$03.00/0

MOLECULAR PHARMACOLOGY, 44:336–345

Interactions of Indolo[3,2-*b*]carbazoles and Related Polycyclic Aromatic Hydrocarbons with Specific Binding Sites for 2,3,7,8-Tetrachlorodibenzo-*p*-dioxin in Rat Liver

MIKAEL GILLNER,[1] JAN BERGMAN, CHRISTIAN CAMBILLAU, MONIKA ALEXANDERSSON, BIRGITTA FERNSTRÖM, and JAN-ÅKE GUSTAFSSON

Department of Medical Nutrition, Karolinska Institute, Huddinge University Hospital F60, NOVUM, S-141 86 Huddinge, Sweden (M.G., M.A., B.F., J.-Å.G.), Department of Organic Chemistry, Royal Institute of Technology, Center for Nutrition and Toxicology, NOVUM, S-14157 Huddinge, Sweden (J.B.), and Laboratoire de Cristallographie et Cristallisation de Macromolecules Biologiques, URA 232, Faculté Nord, 13326 Marseille Cedex 15, France (C.C.)

Received December 30, 1992; Accepted May 4, 1993

SUMMARY

In the present study we have investigated the capacity of various compounds sterically related to indolo[3,2-*b*]carbazole to inhibit specific 2,3,7,8-tetrachloro[1,6-^{3}H]dibenzo-*p*-dioxin binding in rat liver cytosol, as analyzed by electrofocusing in polyacrylamide gels. When the two nitrogen atoms of indolo[3,2-*b*]carbazole (IC_{50} = 3.6 nM) were replaced with sulfur atoms, the affinity for the specific binding sites (IC_{50} = 3.3 nM) was similar to that of the parent compound, whereas the affinity decreased when the two nitrogen atoms were replaced with oxygen atoms (IC_{50} = 29 nM). Substitution with methyl groups at positions 5 and 11 (on the nitrogens) of indolo[3,2-*b*]carbazole resulted in increased affinity (IC_{50} = 1.2 nM), compared with that of the parent compound, whereas dimethylation at the 4,10- or 2,8-positions decreased the affinity (IC_{50} = 19 nM and IC_{50} > 150 nM, respectively). Substitution at positions 5 and 11 of indolo[3,2-*b*]carbazole with substituents larger than methyl, as in 5,11-diethylindolo[3,2-*b*]carbazole (IC_{50} = 8.9 nM), diacetylindolo[3,2-*b*]carbazole (IC_{50} = 11.2 nM), 5,11-dibutylindolo[3,2-*b*]carbazole (IC_{50} > 150 nM), and 5,11-di(*N*,*N*-dimethylaminoethyl)indolo[3,2-*b*]carbazole (IC_{50} > 1500 nM), also decreased the affinity. Introduction of oxygen in, or hydroxylation of, the middle ring of indolo[3,2-*b*]carbazole, giving indolo[3,2-*b*]carbazole-6,12-quinone (IC_{50} > 150 nM) or 6,12-dihydroxyindolo[3,2-*b*]carbazole (IC_{50} > 1500 nM), respectively, also lowered the affinity. We calculated the Gibbs free energy of solvation of the analogue isoquino[3,4-*b*]phenanthridine (IC_{50} = 137 nM), relative to that of dibenz[*a*,*h*]anthracene (IC_{50} = 2.5 nM), in water to be −6 kcal/mol by free energy perturbation, which indicates that the most important explanation for the observed difference in binding affinity is the smaller difference in relative free energy of binding at the binding sites, compared with the Gibbs free energy of solvation of the two compounds.

The *Ah* receptor is currently perceived as a ligand-activated *trans*-acting gene regulatory protein that specifically binds AHH-inducing compounds such as 5,6-benzoflavone and PAHs, e.g., 3-methylcholanthrene and benzo[*a*]pyrene, as well as chlorinated hydrocarbons, e.g., chlorinated dioxins, dibenzofurans, and biphenyls (1–4). Recent results from molecular cloning and cell culture experiments indicate that the *Ah* receptor contains a sequence with homology to the helix-turn-helix motif found in certain DNA-binding proteins such as the human Arnt and *Drosophila* Sim proteins, whereas no sequence homology to DNA-binding proteins containing a zinc-finger motif, e.g., steroid hormone receptors, has been demonstrated (1–3).

Because TCDD is an environmental contaminant of mainly industrial origin, it is unlikely to be a natural ligand for the *Ah* receptor. An endogenous ligand for the *Ah* receptor has not been identified and it is possible that its natural ligand is of exogenous nature. Thus, PAHs from forest fires (and possibly also TCDD, to some extent) have always been present in the

This research was supported by funds from the Karolinska Institute, the Swedish Cancer Society, the National Institutes of Health (Fellowship 1 F05 TW 0446–01), the Swedish Medical Research Council (Grant 09279), the Ekhaga Foundation, and the Swedish National Supercomputing Center.

[1] Present address: University of California, Metabolic Research Unit, 1141 Health Sciences West, San Francisco, CA 94143–0540.

ABBREVIATIONS: *Ah*, aromatic hydrocarbon responsiveness; TCDD, 2,3,7,8-tetrachlorodibenzo-*p*-dioxin; AHH, aryl hydrocarbon hydroxylase; PAH, polycyclic aromatic hydrocarbon; IC_{50}, inhibitory concentration that competes for one-half of the specific binding sites; QSAR, quantitative structure-activity relationship; G_{solv}, Gibbs free energy of solvation of a compound in a liquid (here water) in equilibrium with the gas phase of the same compound (33); ΔG_{solv}, difference in aqueous solvation free energies of two compounds; ΔG_{bind}, difference in Gibbs free energies of two ligand-protein complexes *in vacuo*; $\Delta\Delta G_{bind}$, Gibbs free energy difference in the two ligand-protein complexes in water [related to experimentally determined relative binding affinities of compounds A and B by $\Delta\Delta G_{bind} = RT\ln$($IC_{50}$ for compound B/reference compound A), where R is the gas constant and T is the absolute temperature].

environment. Another possibility is that the natural *Ah* receptor ligand occurs in the diet.

In an earlier study (5) we found that indolo[3,2-*b*]carbazole binds to the *Ah* receptor with high affinity.[2] This heteroaromatic polycycle may be chemically derived *in vitro* (under acidic conditions in the presence of light and a photosensitizer) (6) from some of the indoles, e.g., 3,3′-diindolylmethane and indole-3-carbinol, occurring in Brussels sprouts that were earlier reported to induce AHH (7) and to protect against PAH-induced neoplasia (7). Recent studies do support the notion of an acid-catalyzed formation also *in vivo* of an *Ah* receptor ligand with higher affinity than the carbinol itself (8–10).

It has also been suggested that an endogenous ligand for the *Ah* receptor may be formed after UV irradiation of tryptophan (11, 15). We have shown (12) that dehydrorutaecarpin, which may be chemically derived from tryptamine, binds to the *Ah* receptor with a relatively high affinity (IC_{50} = 7 nM). This implies that desaza analogues of rutaecarpin, which would have the same molecular weight as the most active but as yet unidentified UV-condensation product of tryptophan, constitute candidates for a natural *Ah* receptor ligand.

The hypothesis of dietary tryptophan as a ligand precursor is further supported by recent work by Perdew and Babbs (13), which indicates that gastrointestinal bacteria are capable of metabolizing tryptophan to *Ah* receptor ligands. Because the *Ah* receptor has been detected in the gastrointestinal tract (14), it is possible that AHH and other *Ah* receptor-regulated enzymes in the mucosal cells could be directly modulated by such locally produced compounds.

In light of the continued interest in indoles as precursors of *Ah* receptor ligands, it appears essential to expand our knowledge about structural requirements for the binding of indole condensation products and related heterocyclic compounds to the *Ah* receptor. To accomplish this objective, for the present study we have synthesized or acquired derivatives and analogues of indolo[3,2-*b*]carbazole, examined them by means of receptor binding assays and molecular structure studies, and compared their properties with those of known *Ah* receptor ligands. Furthermore, we applied recent methodology for computation of relative free energies of solvation (16, 17) to two ligands, to account for some of our results that we were unable to interpret on the basis of molecular structure considerations alone.

In this methodology free energy perturbation is applied by the use of molecular dynamics. This methodology, which is briefly outlined in Materials and Methods, may be used to determine a change or "mutation" in any system that can be adequately represented. In the present study the changes studied consist of replacements of atoms in molecules solvated in water.

Materials and Methods

Chemicals. Dibenz[*a*,*h*]anthracene, benz[*a*]anthracene, and 7,12-dimethylbenz[*a*]anthracene were obtained from Sigma Chemical Co. (St. Louis, MO). Benzo[1,2-*b*:4,5-*b*′]bis[1]benzothiophene was a kind gift from Dr. P. Kirby (Shell Co., Sittingbourne Research Centre, Kent, UK). Isoquino[3,4-*b*]phenanthridine was generously provided by Dr. LeRoy H. Klemm (University of Oregon, Eugene, OR). These compounds were used without further purification.

Benzo[1,2-*b*:4,5-*b*′]bisbenzofuran was prepared according to the method of Bergman *et al.* (18). 5,11-Dimethylindolo[3,2-*b*]carbazole was synthesized as described by Hunig and Steinmetzer (19). 2,8-Dimethylindolo[3,2-*b*]carbazole and 4,10-dimethylindolo[3,2-*b*]carbazole were prepared according to the procedure of Robinson (20), with the corresponding phenylhydrazones as starting materials. 5,11-Diacetylindolo[3,2-*b*]carbazole was synthesized as described by Robinson (20). 5,11-Diethylindolo[3,2-*b*]carbazole and 5,11-dibutylindolo[3,2-*b*]carbazole were prepared by alkylation of indolo[3,2-*b*]carbazole according to the method of Bergman and Sand (21). 6,12-Dihydroxyindolo[3,2-*b*]carbazole was prepared by reduction of the corresponding quinone with zinc in acetic acid; the indolo[3,2-*b*]carbazole-6,12-quinone was prepared as described by Osman *et al.* (22). 5,11-Di(*N*,*N*-dimethylaminoethyl)indolo[3,2-*b*]carbazole was prepared according to the method of Bergman.[3] All indolo[3,2-*b*]carbazoles were purified by sublimation under reduced pressure. The compounds synthesized were at least 95% pure, as judged by mass spectrometry. IR spectra of 5,11-dimethylindolo[3,2-*b*]carbazole, 5,11-diethylindolo[3,2-*b*]carbazole, and 5,11-dibutylindolo[3,2-*b*]carbazole were recorded, and no N-H signals were observed, indicating that these preparations contained <0.5% indolo[3,2-*b*]carbazole. Other chemicals were obtained from the same sources as described earlier (5).

Receptor binding studies. As an *Ah* receptor source, rat liver cytosol was used and diluted to a protein concentration of 1–3 mg of protein/ml. All samples were incubated in the presence of 1.5 nM [1,6-^{3}H]TCDD for 2 hr at 2°, and a 200-fold excess of 2,3,7,8-tetrachlorodibenzofuran was used to determine nonspecific binding. Compounds that were insoluble in dimethylsulfoxide at room temperature were dissolved in *N*,*N*-dimethylacetamide. The same volume of *N*,*N*-dimethylacetamide was added to the incubations without competitor. Binding assays were performed by electrofocusing in polyacrylamide gels, and determination of IC_{50} values by logit-log plots was carried out as described earlier (5).

Molecular structure studies. The molecular structure studies were performed as described earlier (5), using crystallographic data from the literature as input data. Coordinates were available for dibenz[*a*,*h*]anthracene (23), 3-methylcholanthrene (24), benz[*a*]anthracene (25), and 7,12-dimethylbenz[*a*]anthracene (26) and were used without modification. The following structures were used as parent compounds: for benzo[1,2-*b*:4,5-*b*′]bisbenzofuran, 6,12-disalicyloylbenzo[1,2-*b*:4,5-*b*′]bisbenzofuran (18); for 2,3,7,8-tetrachlorodibenzofuran, dibenzofuran (27); for 3,3′,4,4′-tetrachlorobiphenyl, 2,2′- dichlorobiphenyl; and for indolo[3,2-*b*]carbazoles and benzo[1,2-*b*:4,5-*b*′]bis[1]benzothiophene, 14-acetylindolo[2,3-*a*:2′,3′-*c*]carbazole. Crystallographic coordinates for the two latter parent compounds were obtained from the same sources as described earlier (5).

The parent structures were modified by transpositions of the molecular fragments when necessary, removal of excess atoms, addition of desired atoms in standard positions, and rotation of the final structure. The van der Waals radii of all atoms were added and images of the molecules were plotted in such a way that the main plane of the molecules coincided with the plotting plane. The van der Waals radii values for the atoms were taken from the work of Pauling (28), as follows (in Å): H, 1.2; O, 1.4; N, 1.5; Cl, 1.8; C, 1.7; S, 1.85.

Free energy perturbation studies. The free energy difference between two states of a system, A and B, can be described as $\Delta G = -RT\ln\langle\exp(-H_{AB}/RT)\rangle_A$, where H_{AB} is the difference in the hamiltonian function (i.e., the sum of all contributors to the total energy) of states A and B, ΔG is the free energy difference between these states, and the symbol $\langle\rangle_A$ indicates that an ensemble average is to be taken over the reference state A. This relationship is implemented computationally to describe the intermediary states between A and B. The perturbation calculations are carried out by specifying the parameters in the beginning and end states, the number of intervals or "windows" between the states, and the length of time for equilibration and data

[2] Indolo[3,2-*b*]carbazole should, according to Chemical Abstracts, be called 5,11-dihydroindolo[3,2-*b*]carbazole.

[3] J. Bergman, unpublished observations.

collection in each window. In the present study the slow growth method was used, which is the limiting case of the windowing methodology (i.e., infinitesimally small steps/windows without intermediary equilibrations), and it is assumed that the change is effected so slowly that the system is practically at equilibrium at each step. The program automatically carries out the gradual transformation between the two states A and B by incrementally changing the coupling parameter λ (for state A at the outset, the "mother compound," λ = 1 and finally for state B, the "mutant compound," with 0% A character and 100% B character, λ = 0). During this transformation intermediate energy values are accumulated, stored, and reported for each window as $\Delta G = \Sigma[G(\lambda + \Delta\lambda) - G(\lambda)]$.

Two calculations are sufficient to theoretically completely derive the relative free energy of protein binding of two different ligands. The first one determines the aqueous solvation free energy difference between the two ligands (ΔG_{solv}), and the second determines the free energy difference in the two ligand-protein complexes (ΔG_{bind}). Because the free energy is a state function (i.e., the difference in energy between two states is independent of the path chosen between them), the difference ($\Delta G_{bind} - \Delta G_{solv}$) is equal to the difference in aqueous solution binding free energies of the two inhibitors ($\Delta\Delta G_{bind}$), according to Fig. 1. For free energy calculations the molecular simulation program Amber 4.0[4] was used and for *ab initio* calculations Gaussian-92[5] was used. Both programs were run on a Cray computer. To benzene the same force-field parameters (except for the van der Waals parameters for the sp^2-carbon C_A, where $R^* = 1.85$ Å and $\epsilon = 0.12$ kcal/mol were used) and charges (in electron units, q_e) (C_A, −0.14; H_C, 0.14) were applied as used in earlier studies (17). Extra charges [derived at the 6–31G* level as described by Bash *et al.* (17), from the 6–31G* geometry without fit or scaling to the electric dipole moment, using Gaussian-92] and required parameters used for pyridine were, for charges: D_H, 0.0; N_C, −0.68; *o*-C_Q, 0.46; *o*-H_C, 0.04; *m*-C_A, −0.52; *m*-H_C, 0.20; *p*-C_A, 0.22; *p*-H_C, 0.1 for mass of dummy hydrogen (in units); $D_H = 1.008$; N_C-D_H, $K_r = 340$, $r_{eq} = 1.08$; C_A-C_Q, $K_r = 469$, $r_{eq} = 1.38$; C_Q-N_C-C_Q, $K_\theta = 70$, $\theta_{eq} = 117.7$; N_C-C_Q-C_A, $K_\theta = 70$, $\theta_{eq} = 123.6$; C_A-C_A-C_Q, $K_\theta = 70$, $\theta_{eq} = 118.2$; C_Q-N_C-D_H, $K_\theta = 35$, $\theta_{eq} = 120.0$; C_Q-C_A-H_C, $K_\theta = 35$, $\theta_{eq} = 120.3$; C_A-C_Q-H_C, $K_\theta = 35$, $\theta_{eq} = 120.3$; X-C_A-C_Q-X, $V_n/4 = 3.7$, $\gamma = 180$, $\eta = 2$. One additional bond angle parameter (C_A-C_Q-C_A, $K_\theta = 70$, $\theta_{eq} = 120.3$) was needed for isoquino[3,4-*b*]phenanthridine, and for dibenz[*a*,*h*]anthracene the benzene parameters were sufficient. The charges for the two latter compounds were also derived on the 6–31G* level, as described above, with the optimized 6–31G* structure of isoquino[3,4-*b*]phenanthridine and with a partially optimized (from the optimized 6–31G structure at the 6–31G* level) structure of dibenz[*a*,*h*]anthracene, respectively.

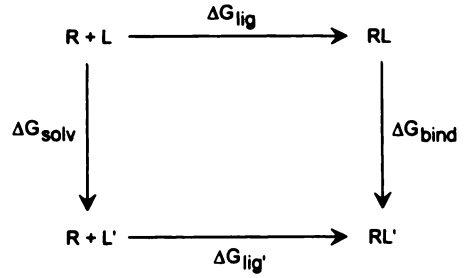

Fig. 1. Scheme for a thermodynamic cycle describing receptor-ligand binding in solution. In this cycle ΔG_{solv} is the difference in Gibbs free energy of solvation between the ligands L and L′, ΔG_{bind} is the difference in free energy of binding between L and L′ at the binding site of the receptor (R), and ΔG_{lig} and $\Delta G_{lig'}$ are the free energies of receptor binding of the ligands L and L′, respectively. It is currently not possible to directly simulate the ΔG_{lig} and $\Delta G_{lig'}$ terms, but it is possible to simulate the transitions L to L′ in solution and (provided that the three-dimensional structure of the receptor is available) in the protein.

For the calculation of relative free energies of solvation, the ligand to be changed was placed in a box of water molecules (354 for benzene, 344 for pyridine, and 533 for dibenz[*a*,*h*]anthracene) generated by Monte-Carlo simulation. The systems were initially partially minimized for 200 steps and equilibrated by molecular dynamics performed at constant temperature (300°K) and pressure (1 atm) using periodic boundary conditions (during 5 psec for pyridine and benzene and during 20 psec for isoquino[3,4-*b*]phenanthridine). A cut-off of 8 Å was used for the nonbonded pair-list, which was updated every fifth time-step ($\Delta t = 0.001$ psec), and the SHAKE algorithm was used to constrain bonds involving hydrogens to their equilibrium values. After pre-equilibration the systems were perturbed to obtain the free energy difference of the A to B transition as described by Bash *et al.* (17), using the same conditions as for the pre-equilibrations. Slow growth simulations were performed without decoupling of the electrostatic contributions from the van der Waals contributions to the ΔG.

Results

We have studied various possible *Ah* receptor ligands by means of molecular structure studies and receptor binding assays. IC_{50} values for various compounds for their inhibition of specific [^{3}H]TCDD binding in rat liver cytosol are listed in Table 1, and their structural formulas are shown in Fig. 2.

Because methylation in a critical position is known to increase the affinity of some steroids for their receptors, it was of interest to investigate the effect on receptor affinity exerted by methylation of indolo[3,2-*b*]carbazole (IC_{50} = 3.6 nM) at various positions. *N*-Methylation of the indolo[3,2-*b*]carbazole, leading to 5,11-dimethylindolo[3,2-*b*]carbazole (**I**), increased the affinity about 3-fold (IC_{50} = 1.2 ± 0.2 nM), compared with the parent structure, indolo[3,2-*b*]carbazole (**IV**).

Based on the assumption that there may be steric features in common for high affinity ligands for the *Ah* receptor that are not present in low affinity ligands, we created computer-generated plots of images of some receptor-binding molecules (shown in Fig. 3). Because the affinity of 5,11-dimethylindolo[3,2-*b*]carbazole (Fig. 3D) was higher than that of its parent compound, indolo[3,2-*b*]carbazole (Fig. 3B), we also fitted the ligands shown in Fig. 3 (with the van der Waals radii of all atoms included) into a 6.8- × 13.7-Å rectangle designed to fit 5,11-dimethylindolo[3,2-*b*]carbazole, with a protrusion 2.2-Å long and 3.0-Å wide situated on the long side at a distance of 3.0 Å from its corner. As evident from the plot (Fig. 3D) and the symmetry of the molecule, either of the methyl groups of 5,11-dimethylindolo[3,2-*b*]carbazole fits into the protrusion. On the other hand, we found that 4,10-dimethylindolo[3,2-*b*]carbazole (**VII**) and 2,8-dimethylindolo[3,2-*b*]carbazole (**XIII**), where the methyl groups do not fit into the protrusion, had lower affinities (IC_{50} = 19 ± 5 nM and IC_{50} > 150 nM, respectively) for the rat liver *Ah* receptor than did the parent compound.

Because it is known that the halogens are necessary for the receptor binding of halogenated dioxins, dibenzofurans, and biphenyls (29), we wanted to investigate whether the nitrogens were of similar importance for receptor binding of the indolo[3,2-*b*]carbazole parent structure. We therefore studied the isosteric heterocycles where both nitrogens of indolo[3,2-*b*]carbazole are replaced by sulfur or oxygen atoms. Benzo[1,2-*b*:4,5-*b*′]bis[1]benzothiophene (**III**) (Fig. 3A) has a larger heteroatomic van der Waals radius (1.85 Å) (28) and covalent

[4] Program available from Dr. Peter Kollman, Department of Pharmaceutical Chemistry, UCSF, San Francisco, CA 94143–0446.
[5] Program available from Gaussian Inc, 4415 5th Ave., Pittsburgh, PA 15213.

TABLE 1

Names and capacities of indolo[3,2-*b*]carbazole and analogues to inhibit specific binding of [^{3}H]TCDD in rat liver cytosol

Assays were performed as outlined in Materials and Methods, and IC_{50} values were calculated as described earlier (5). Correlation coefficients for linear regression were generally above 0.9 for competitors with IC_{50} values below 150 nM. IC_{50} values for inhibition of specific [^{3}H]TCDD binding represent the mean ± standard deviation from three separate experiments. Roman numerals refer to structures of compounds shown in Fig. 2. Projections of the molecules are plotted in Fig. 3.

Compound	Name	IC_{50}
		nM
I	5,11-Dimethylindolo[3,2-*b*]carbazole (Fig. 3D)	1.2 ± 0.2
II	Dibenz[*a*,*h*]anthracene (Fig. 3G)	2.5 ± 0.7
III	Benzo[1,2-*b*:4,5-*b*′]bis[1]benzothiophene[a,b] (Fig. 3A)	3.3 ± 2.2
IV	Indolo[3,2-*b*]carbazole[c] (Fig. 3B)	3.6 ± 2.6
V	5,11-Diethylindolo[3,2-*b*]carbazole[a] (Fig. 3E)	8.9 ± 4.2
VI	5,11-Diacetylindolo[3,2-*b*]carbazole (Fig. 3F)	11.2 ± 5.2
VII	4,10-Dimethylindolo[3,2-*b*]carbazole	19 ± 5
VIII	Benzo[1,2-*b*:4,5-*b*′]bisbenzofuran[a] (Fig. 3C)	29 ± 10
IX	Benz[*a*]anthracene (Fig. 3I)	48 ± 6
X	Isoquino[3,4-*b*]phenanthridine[a]	137 ± 26
XI	7,12-Dimethylbenz[*a*]anthracene (Fig. 3J)	139 ± 6
XII	5,11-Dibutylindolo[3,2-*b*]carbazole	>150
XIII	2,8-Dimethylindolo[3,2-*b*]carbazole	>1500
XIV	5,11-Di(*N*,*N*-dimethylaminoethyl)indolo[3,2-*b*]carbazole	>1500
XV	Indolo[3,2-*b*]carbazole-6,12-quinone	>150
XVI	6,12-Dihydroxyindolo[3,2-*b*]carbazole	>1500

[a] Because of their limited solubility, these competitors were dissolved in *N*,*N*-dimethylacetamide instead of dimethylsulfoxide, as described in Materials and Methods, before addition to the incubations.

[b] The IC_{50} value of benzo[1,2-*b*:4,5-*b*′]*bis*[1]benzothiophene was decreased if the same solution was used the next day, indicating an instability of this compound in solution. Possibly this may be due to uptake of oxygen and formation of the corresponding sulfone.

[c] Determined earlier (5).

bond length (1.04 Å) (28) than does indolo[3,2-*b*]carbazole (Fig. 3B), which has a heteroatomic van der Waals radius of 1.5 Å and covalent bond length of 0.7 Å (28). This sulfur isoster of indolo[3,2-*b*]carbazole therefore has somewhat more bulk at the site of the protrusion, as visualized in Fig. 3A [compared with indolo[3,2-*b*]carbazole, also when the volume of the hydrogen atoms (van der Waals radius, 1.2 Å; covalent bond length, 0.3 Å) (28) on its nitrogen atoms is considered] and a somewhat higher, or similar, receptor affinity (IC_{50} = 3.3 ± 2.2 nM). The affinity of the oxygen analogue benzo[1,2-*b*:4,5-*b*′]bisbenzofuran (**VIII**) for the *Ah* receptor was lower (IC_{50} = 29 ± 10 nM) than that of indolo[3,2-*b*]carbazole. The furan oxygen has a smaller van der Waals radius (1.4 Å) and a shorter covalent bond length (0.66 Å) (18) than do the indole nitrogens of indolo[3,2-*b*]carbazole and therefore benzo[1,2-*b*:4,5-*b*′]bisbenzofuran has less volume at the site of the protrusion (especially if the volume of the hydrogens on the nitrogens of indolo[3,2-*b*]carbazole is considered), as visualized in Fig. 3C.

Because methylation at positions 5 and 11 of indolo[3,2-*b*]carbazole was found to increase the receptor affinity, compared with that of the parent compound, it was of interest to investigate the effects of other substituents at these positions. Although the data set is too limited to perform a strict QSAR analysis, we have presented in Table 2 values of various parameters commonly used in QSAR of substituent effects, for the 5,11-substituted indolo[3,2-*b*]carbazoles we have been able to synthesize. *N*-Ethylation of indolo[3,2-*b*]carbazole, leading to 5,11-diethylindolo[3,2-*b*]carbazole (**V**) (Fig. 3E), decreased the binding affinity by a factor of 3 (IC_{50} = 8.9 ± 4.2 nM), compared with the parent compound. Substitution on the nitrogens of indolo[3,2-*b*]carbazole with more bulky substituents, such as an acetyl group as in 5,11-diacetylindolo[3,2-*b*]carbazole (**VI**) (Fig. 3F) or a butyl group as in 5,11-dibutylindolo[3,2-*b*]carbazole (**XII**), further decreased the affinity (IC_{50} = 11.2 ± 5.2 nM and IC_{50} > 150 nM, respectively). These results may be interpreted as if a maximum size of the 5,11-substituent has been exceeded by these ligands and/or as if larger substituents than methyl interfere with planarity, because they may stick out from the main plane of the molecule. The affinity of 5,11-di(*N*,*N*-dimethylaminoethyl)indolo[3,2-*b*]carbazole (**XIV**), with very bulky *N*-substituents, was also reduced (IC_{50} > 1500 nM).

Of the QSAR parameters for 5,11-substituents of six indolo[3,2-*b*]carbazoles in Table 2, the molecular refractivity appeared to be most correlated with the *Ah* receptor affinity (log IC_{50}) for methyl substituents and larger substituents. Molecular refractivity is dependent on the size and polarizability of the substituent (30).

When indolo[3,2-*b*]carbazole was hydroxylated in the middle ring, as in 6,12-dihydroxyindolo[3,2-*b*]carbazole (**XVI**), the receptor affinity was reduced by 2 orders of magnitude (IC_{50} > 1500 nM). The affinity of the corresponding quinone (**XV**) for the *Ah* receptor was also found to be low (IC_{50} > 1500 nM).

Either of the two K-regions (31) of dibenz[*a*,*h*]anthracene (**II**) (IC_{50} = 2.5 ± 0.7 nM), which has a high affinity for the mouse liver *Ah* receptor (32), may be fitted into the protrusion, as is evident from Fig. 3G. Hence, we proceeded to regard some other PAHs as imperfect dibenz[*a*,*h*]anthracene analogues and oriented the phenanthrene part of their ring system in the same manner as the K-region of dibenz[*a*,*h*]anthracene that is not fitted into the protrusion.

The ring with the methyl substituent of 3-methylcholanthrene (which has an affinity for the mouse liver *Ah* receptor intermediary between those of benz[*a*]anthracene and 5,6-benzoflavone) (33) partially fills the protrusion (Fig. 3H). Although the corresponding rings of benz[*a*]anthracene (**IX**) (IC_{50} = 48 ± 6 nM; Fig. 3I), and 7,12-dimethylbenz[*a*]anthracene (**XI**) (IC_{50} = 139 ± 6 nM; Fig. 3J) partially fill the protrusion when oriented as shown in Fig. 3, the affinity of these PAHs is 1 order of magnitude lower than that of dibenz[*a*,*h*]anthracene. Probably a critical molecular size must be attained by ligands for high affinity binding. Although the explanation for the

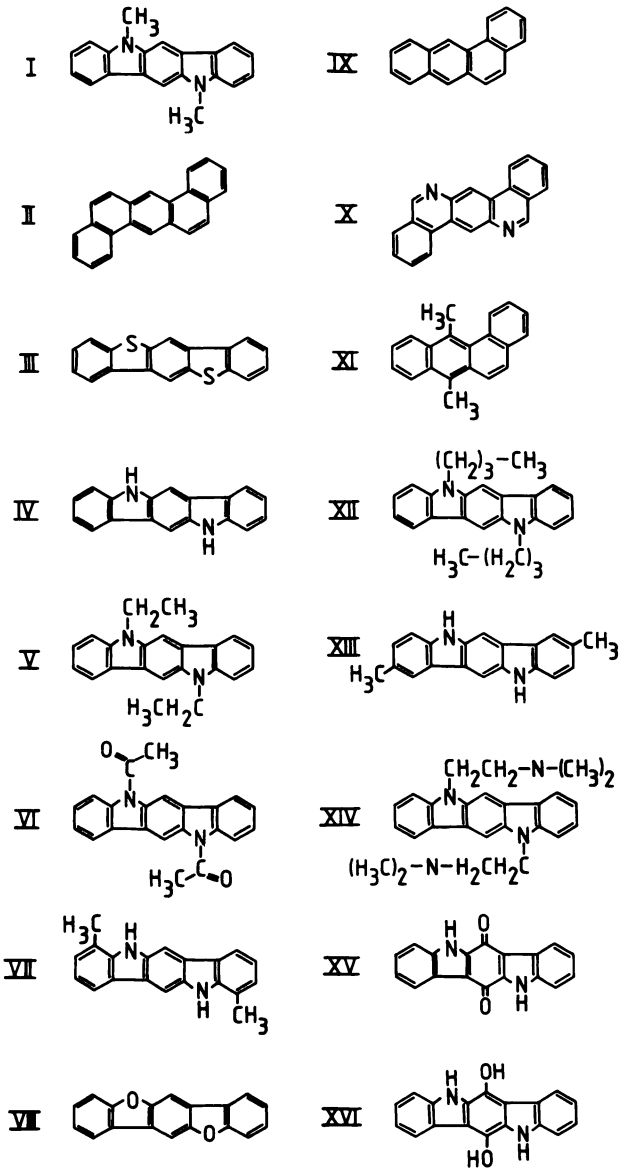

Fig. 2. Structural formulas for the competitors used to inhibit specific [^{3}H]TCDD binding in rat liver cytosol. *Roman numerals* refer to the names of compounds in Table 1.

lower affinity of 7,12-dimethylbenz[*a*]anthracene may be more complex than can be accounted for by steric factors alone, the generalization that planarity is required for molecules interacting with the *Ah* receptor (4) is not refuted by the results for the PAH ligands studied here, because the 7,12-dimethylbenz[*a*]anthracene molecule is nonplanar (26).

To gain a perspective on why the dibenz[*a*,*h*]anthracene analogue isoquino[3,4-*b*]phenanthridine (X) had a much lower affinity (IC_{50} = 137 ± 26 nM) than did dibenz[*a*,*h*]anthracene, although the two compounds are approximately isosteric, we carried out free energy perturbation calculations to determine their relative free energy of solvation in water. Initially we carried out pilot calculations on the model compounds benzene (reference) and pyridine (Table 3), to validate our system. The interaction energy of the ligand with the solvent at values of its parameters (designated F for $\lambda + \Delta\lambda$ and R for $\lambda - \Delta\lambda$ in Table 3) provided an internal check of the method, because the sum of these two energy changes over all intervals should be the same. To obtain an estimate of the statistical error for the simulation by independent simulations for the same systems, we carried out a second simulation for the backward B to A transition, starting from the final coordinates from the forward A to B simulation. The dependency of the starting configuration, which may be appreciated as the degree of hysteresis (i.e., degree of thermodynamic reversibility), appears to be small, as judged from the plot of ΔG_{solv} versus λ shown in Fig. 4. The mean from the calculations in both directions was −3.0 ± 0.1 kcal/mol (Table 3), which is in line with the experimental data for the solvation in water from the gas phase of pyridine, compared with benzene (ΔG_{solv} = −3.8 kcal/mol) (34).

There is not yet any rule of thumb established to determine whether a free energy perturbation calculation is converged with respect to increasing time spans of the simulation. To establish that the time used for the simulation (40 psec) was adequate, we also perturbed pyridine to benzene during 40 psec and repeated the same calculation using doubled as well as quadrupled simulation lengths (depicted in Fig. 5). Because the result does not appear to be critically dependent on the length of the simulation (as can be seen in Table 3) the perturbations of dibenz[*a*,*h*]anthracene/isoquino[3,4-*b*]phenanthridine were also carried out using a simulation length of 40 psec. To derive the necessary point charges for the latter perturbation, we fitted the electrostatic potential calculated at the 6–31G* level to the atomic van der Waals radii of the molecules (Fig. 6). The latter perturbations resulted in a ΔG_{solv} of −6.2 ± 0.1 kcal/mol for isoquino[3,4-*b*]phenanthridine, compared with dibenz[*a*,*h*]anthracene (Table 3), again with an apparently small hysteresis (Fig. 7).

Discussion

The indolocarbazoles, as well as some other isosteric heterocycles studied in this work, represent a class of *Ah* receptor ligands distinct from the other known ligands (halogenated aromatic hydrocarbons and PAHs). The *Ah* receptor-binding estimates of these heterocycles may therefore be of value for development of more general structure-affinity concepts than those presently available for binding of ligands to the *Ah* receptor.

The nitrogens of indolo[3,2-*b*]carbazole (IV in Table 1) do not seem necessary for *Ah* receptor binding of this parent structure, because the corresponding heterocycles where the nitrogens are replaced by oxygen or sulfur also have appreciable receptor affinity.

The *Ah* receptor affinity of the investigated methylated indolo[3,2-*b*]carbazoles is in the rank order 5,11-dimethyl > 4,10-dimethyl > 2,8-dimethyl, i.e., the receptor affinity decreases with increasing distance between the methyl groups and nitrogen atoms. These results also indicate that the 5 (or 11)-position probably is the optimal site for affinity-increasing substitution (of the ones we were able to investigate) of indolo[3,2-*b*]carbazoles (and possibly also for other molecules approximately isosteric to indolocarbazoles with respect to the atomic van der Waals radii), because only methylation at these sites was found to increase the receptor affinity of indolo[3,2-*b*]carbazole.

The observation that 5,11-substituents larger than methyl groups on indolo[3,2-*b*]carbazole tend to decrease, rather than increase, the affinity of the ligand for the *Ah* receptor indicates that this size of substituent is nearly optimal. The observation

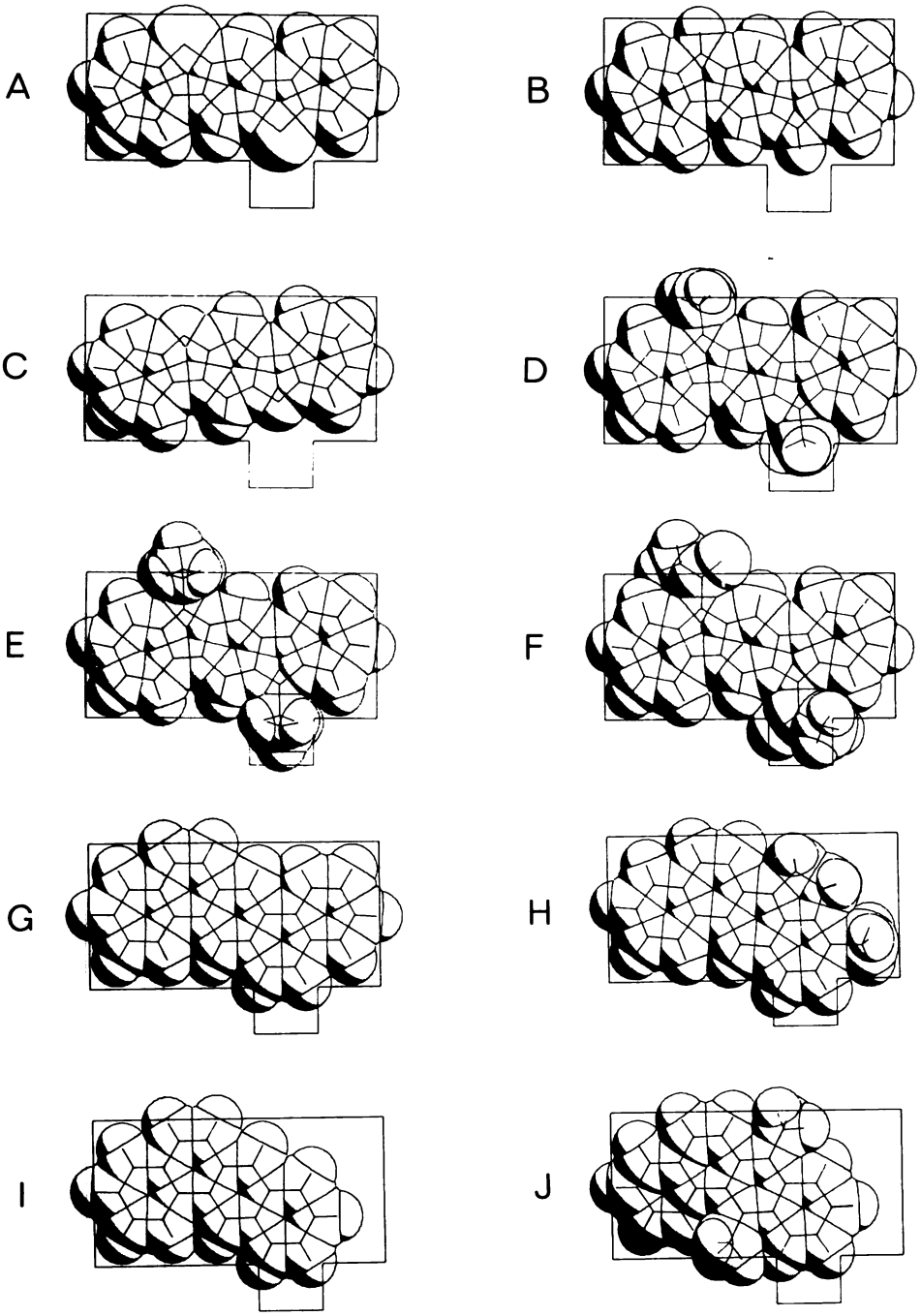

Fig. 3. Images of some *Ah* receptor-binding heterocyclic molecules with van der Waals radii included. The images were built from crystallographic data, with the van der Waals radii according to Pauling (28) being added by means of a computer, and were plotted as outlined in Materials and Methods. The outer rectangle is 6.8 Å × 13.7 Å, with a 2.2 × 3.0 Å protrusion on the long side, 3.0 Å from the corner accommodating certain affinity-increasing substituents. Plots are shown for benzo[1,2-*b*:4,5-*b'*]bis[1]benzothiophene (A), indolo[3,2-*b*]carbazole (B), benzo[1,2-*b*:4,5-*b'*]bisbenzofuran (C), 5,11-dimethylindolo[3,2-*b*]carbazole (D), 5,11-diethylindolo[3,2-*b*]carbazole (E), 5,11-diacetylindolo[3,2-*b*]carbazole (F), dibenz[*a*,*h*]anthracene (G), 3-methylcholanthrene (H), benz[*a*]anthracene (I), and 7,12-dimethylbenz[*a*]anthracene (J).

that only the steric QSAR parameters in this (Table 2) and an earlier study of PAHs (35) were correlated with *Ah* receptor affinity also seems to stress the importance of steric factors for ligand binding to the receptor.

Our earlier model of a 6.8- × 13.7-Å rectangle including the molecular atomic van der Waals radii obviously represents a more general concept for binding of ligands to the *Ah* receptor than does the 3- × 10-Å rectangle with the centers of halogen atoms in its corners proposed by Poland and Knutson (4), because the latter accounts only for *Ah* receptor binding of halogenated dioxins and isosteric halogenated ligands, whereas our pattern accounts for the binding of PAH and heterocycles in addition to chlorinated ligands (5).

However, the notion of simplistic patterns that can accommodate good ligands should not be carried too far to try to account for *Ah* receptor ligand binding, because all of the space surrounding known ligands has not yet been probed by substitutions and therefore we cannot establish whether fits into our patterns [our 6.8- × 13.7-Å rectangle without (5) or with a protrusion 2.2-Å long and 3.0-Å wide situated on the long side at a distance 3.0 Å from its corner, as in Fig. 3] are necessary requirements for binding. Furthermore, the binding site may be expected to be more complex, i.e., constituted of amino acids with more or less flexible side chains, which may impose more or less strict steric restrictions in various positions on ligands for their high affinity binding. Thus, examples may be found of compounds, such as dibenz[*a*,*c*]anthracene (32), that despite their lack of fit to either of the mentioned patterns (Poland's or ours) have a relatively high *Ah* receptor affinity. Moreover, examples may be found of compounds, such as chloromethyl-

TABLE 2

Substituent parameters of indolo[3,2-*b*]carbazoles substituted at the 5- and 11-positions

Descriptors shown are σ_m and σ_p for electronic effects, E_s for steric effect, L for length, B_y for width, molecular refractivity (MR) for volume, π for lipophilicity, and log IC_{50} for ^{19}log IC_{50}. σ = log K_X − log K_H, where K_H is the ionization constant of benzoic acid in water and K_X that of substituted benzoic acid, $_m$ = in meta-position, $_p$ = in para-position (positive sign indicates electron withdrawal by the substituent). MR = $((n^2 - 1)/(n^2 + 1))$ (MW/d) where n is the index of refraction, MW the molecular weight, and d is density. π = log P_h − log P_H, where P_H is the partioning coefficient for benzene in water/octanol and PX is that for a substituted benzene. Only steric parameters, e.g., molecular refractivity, seem to be correlated with binding affinity. Substituent values were taken from Ref. 30.

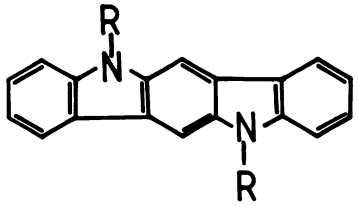

Substituent	σ_m	σ_p	E_s	L	B_y	MR	π	log IC_{50}
R = H	0	0	0	2.06	1	1.03	0	0.556
R = CH_3	−0.07	−0.17	−1.24	3.00	2.04	5.65	0.56	0.078
R = CH_2CH_2	−0.07	−0.15	−1.31	4.11	2.97	10.3	1.02	0.949
R = $COCH_3$	0.38	0.50	−2.0[a]	4.06	2.83	11.18	−0.55	1.049
R = $(CH_2)_3CH_3$	−0.08	−0.16	−1.63	6.17	4.42	19.59	2.13	2.7
R = $(CH_2)_2N(CH_3)_2$	−0.80	−0.16	−3.0[b]	5.58	2.97	22.0[c]	0.41[d]	3.7

[a] Estimated from -CHO.
[b] Estimated from $-CH_2C(CH_3)_3$.
[c] Estimated from pentyl.
[d] Estimated from $-CH_2N(CH_3)_2$.

TABLE 3

Relative free energies of solvation in water for CH to N perturbations of model and ligand compounds computed from the simulations depicted in Figs. 4, 5, and 7

In the first simulation the reference benzene (A, λ = 1) was perturbed to pyridine (B, λ = 0). In the second set of simulations pyridine was perturbed to benzene using different time spans. In the last simulation dibenz[*a*,*h*]anthracene was perturbed to isoquino[3,4-*b*]phenanthridine. The first and last simulations were also carried out in the reverse direction, and for them the ΔG_{solv} was calculated as mean ± standard deviation (two experiments) of both the A to B and B to A simulations.

Reference (A)	Time	Direction[a]	G_{solv} A→B	G_{solv} B→A	ΔG_{solv}[b]
	psec		kcal/mol		kcal/mol
Benzene	40	F	2.916	3.099	
		R	−2.916	−3.099	−3.01 ± 0.13
Pyridine	40	F	−2.999		
		R	2.999		3.00
	80	F	−3.122		
		R	3.122		3.12
	160	F	−2.817		
		R	2.817		2.82
Dibenz[*a*,*h*]anthracene	40	F	6.193	6.286	
		R	−6.192	−6.285	−6.24 ± 0.07

[a] F and R represent the free energies computed in the direction λ → λ + Δλ for the process of λ increasing from 0 to 1 and in the direction λ → λ − Δλ for the process of λ decreasing from 1 to 0, respectively.
[b] All ΔG_{solv} values refer to the process of λ decreasing from 1 to 0.

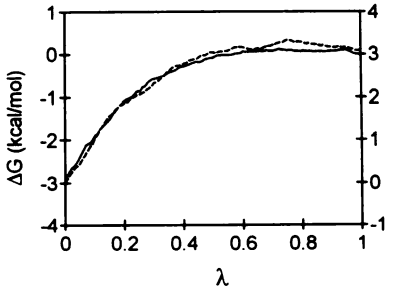

Fig. 4. Cumulative change in Gibbs free energy upon solvation of pyridine, relative to benzene, in water. The dependency of the relative Gibbs free energy of solvation in water (ΔG_{solv}) on λ is shown to illustrate the degree of hysteresis (i.e., degree of thermodynamic reversibility) of the perturbation. Slow growth simulations were performed, each with 40,000 steps at Δt = 0.001 psec, for the transformation of benzene to pyridine in both the forward (——, *left scale*) and reverse (– – –, *right scale*) directions. The system was equilibrated for 5 psec using molecular dynamics, under the same conditions as used for the perturbations, before both the forward and reverse simulations.

dibenzo-*p*-dioxins, that can be fitted into both of the mentioned patterns but have virtually no activity, thus indicating that neither of these patterns describes sufficient requirements for high affinity binding. Whether and how these patterns are reflections of the disposition of amino acids in the binding site of the *Ah* receptor will not be known until the three-dimensional structure of the receptor is solved. Probably other factors (36), such as hydrophobicity of the ligands, are also important determinants for *Ah* receptor binding.

Recent developments in and applications of free energy perturbation methods have emphasized the fact that if the relative differences in free energy in receptor binding of ligands are small relative to the differences in free energy of solvation the latter determines the strength of the ligand-receptor interaction (37). In other words, if the binding site is conceived as being delineated with exclusively, or predominantly, hydrophobic amino acids, the less water soluble the ligand is the more strongly it will bind to the receptor. This does not appear to be an unrealistic assumption, because most high affinity ligands for the *Ah* receptor (e.g., TCDD, PAHs, and indolo[3,2-*b*]carbazole) (38) are almost insoluble in water, i.e., are very hydrophobic and do not appear to contain any obvious hydrogen bond donors or acceptors.

Because isoquino[3,4-*b*]phenanthridine fulfills the steric requirements for high affinity binding suggested here to about the same extent as does dibenz[*a*,*h*]anthracene, the decrease in binding affinity caused by the replacement of carbons with nitrogens would be surprisingly large if only steric factors governed the binding.

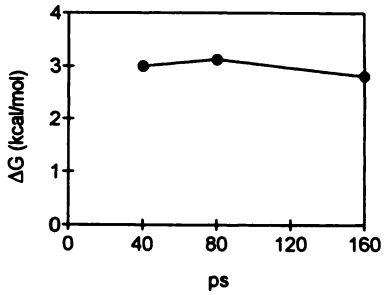

Fig. 5. Dependency of ΔG_{solv} on the time span of the simulation. The dependency of the relative Gibbs free energy of solvation in water on the time of the simulation is shown. Three slow growth simulations were performed in the forward direction, for 40,000, 80,000, and 160,000 steps at Δt = 0.001 psec for the transformation of pyridine to benzene. The system was pre-equilibrated for 5 psec using molecular dynamics under the same conditions as for the perturbations and was then used as a starting conformation for all three simulations.

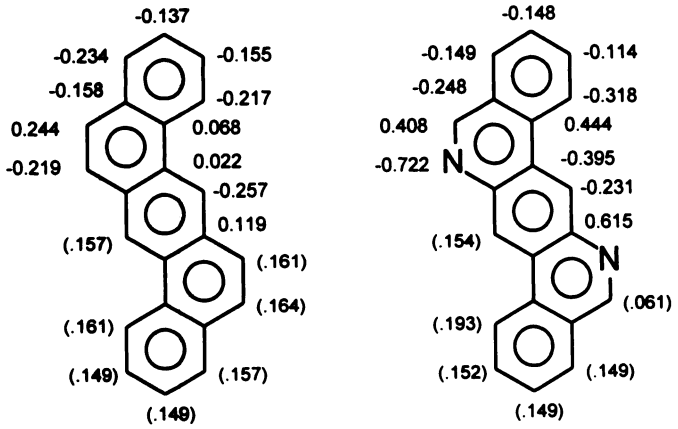

Fig. 6. Partial charges determined with electrostatic potential fitting to the molecular atomic van der Waals surfaces with the use of a 6–31G* basis set for dibenz[*a,h*]anthracene (*left*) and isoquino[3,4-*b*]phenanthridine (*right*). The means of charges on symmetry-equivalent atoms are shown. *Values in parentheses*, hydrogen atom charges.

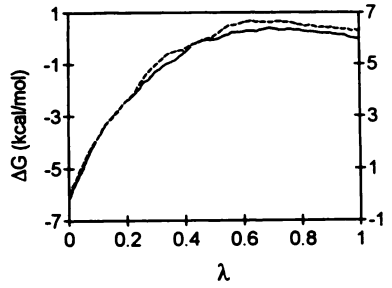

Fig. 7. Cumulative change in Gibbs free energy upon solvation of isoquino[3,4-*b*]phenanthridine, relative to dibenz[*a,h*]anthracene, in water. The dependency of the relative Gibbs free energy of solvation in water (ΔG_{solv}) on λ is shown to illustrate the degree of hysteresis (i.e., degree of thermodynamic reversibility) of the perturbation. Slow growth simulations were performed, each with 40,000 steps at Δt = 0.001 psec, for the transformation of dibenz[*a,h*]anthracene to isoquino[3,4-*b*]phenanthridine in both the forward (——, *left scale*) and reverse (– – –, *right scale*) directions. The system was equilibrated for 20 psec using molecular dynamics, under the same conditions as used for the perturbations, before both the forward and reverse simulations.

The lone-pair electrons of the nitrogen atom of isoquinoline are not delocalized in the π aromatic system but are present in an orbital that has a large proportion of σ character. Therefore, isoquinoline may be expected to be a much stronger base than indole. The pK_a (39) for isoquinoline (5.40) in water is similar to that of pyridine (pK_a = 5.23). Phenanthridine (which is closest to isoquino[3,4-*b*]phenanthridine with respect to structure) is a somewhat weaker base (pK_a = 4.5) (40) than pyridine but a much stronger base than indole (pK_a = −2.4) and a much weaker base than a typical aliphatic amine (e.g., trimethylamine, pK_a = 9.7) (39). These differences in basicity of pyridine, isoquinoline, and phenantridine, compared with indole, is a reflection of the ability of the pyridine (-type) nitrogen atom to accept hydrogen bonds from water (34). Thus, the nitrogens introduced in each of the K-regions of dibenz[*a,h*]anthracene (leading to isoquino[3,4-*b*]phenanthridine) should be more easily protonated than the indolic nitrogens of indolo[3,2-*b*]carbazole. However, at neutral pH (as used in our assay) they should not be protonated.

Our computational result on the relative free energy of solvation (ΔG_{solv} = −6 kcal/mol) of isoquino[3,4-*b*]phenanthridine, compared with dibenz[*a,h*]anthracene, corresponds to a >10,000-fold increased "water affinity" due to the replacement of two CH units by pyridine-type nitrogen atoms. The experimentally measured relative binding affinities of the two compounds are related to $\Delta\Delta G_{bind}$ (the difference in aqueous solution binding free energies of the two ligands). $\Delta\Delta G_{bind}$, is in addition to ΔG_{solv}, dependent on ΔG_{bind} (the free energy difference in the two ligand-protein complexes), which we will not be able to calculate directly using free energy perturbation methods until the three-dimensional structure of the *Ah* receptor becomes available. If we instead derive ΔG_{bind} as $\Delta\Delta G_{bind}$ + ΔG_{solv}, where we use $\Delta\Delta G_{bind} = RT\ln(IC_{50}$ for isoquino[3,4-*b*]phenanthridine/IC_{50} for dibenz[*a,h*]anthracene) = 2.17 kcal/mol from our receptor binding assays, we obtain a ΔG_{bind} of −4 kcal/mol. This indicates that the observed difference in *Ah* receptor binding affinity between isoquino[3,4-*b*]phenanthridine and dibenz[*a,h*]anthracene is dominated by the larger (compared with ΔG_{bind}) relative difference in free energy of solvation in water (ΔG_{solv}) of the two compounds.

One way to interpret the above result is that the difference in receptor affinity observed may be due to a higher degree of hydrophobicity of dibenz[*a,h*]anthracene, compared with isoquino[3,4-*b*]phenanthridine. It should then be remembered that the ΔG_{solv} values computed here by free energy perturbation refer to the relative free Gibbs energies for the transfer of the compounds directly from the gas phase to the liquid phase, whereas hydrophobicity of a compound is often estimated from the relative partitioning of the compound between an organic solvent (e.g., octanol) and water. To completely simulate the latter process using free energy perturbation (which we have not done in the present study) the relative free energies for the transfer of the compounds from the gas phase to the organic solvent must also be computed, as described by, for example, Jorgensen *et al.* (41).

The greatly reduced receptor affinity of 6,12-dihydroxyindolo[3,2-*b*]carbazole, compared with that of the parent compound, is consistent with the observations that various epoxide and diol metabolites of benzo[*a*]pyrene have binding affinities for the *Ah* receptor that are reduced by 2 orders of magnitude, compared with those of their parent compound.[6] The fact that Bash *et al.* (17) obtained $\Delta\Delta G_{solv}$ of −4.57 for phenol with benzene as a reference, using free energy perturbation, supports

[6] J. Carlstedt-Duke, personal communication.

the interpretation that hydroxylation decreases the receptor binding affinity due to a more favorable solvation energy of the product.

Another property that has been proposed as a determinant for *Ah* receptor-mediated biological activity is the presence and strength of negative potentials in certain regions of halogenated dibenzo-*p*-dioxins (42). Unfortunately, it is not immediately clear how to apply this concept to, for example, β-naphthoflavone (43).

Ah receptor binding of halogenated biphenyls and dioxins has also been correlated with polarizability and stacking parameters (44). If polarizability is also important for *Ah* receptor binding of heterocycles, the relatively low affinity of the indolo[3,2-*b*]carbazole-6,12-quinone, compared with indolo[3,2-*b*]carbazole, may possibly be partly due to the fact that a smaller number of π electrons are available in the ring system of the molecule. Furthermore, the rank order of affinities for the *Ah* receptor of the resulting heterocycles when the nitrogens of indolo[3,2-*b*]carbazole are replaced by sulfur or oxygen (S ≥ N > O) approximately parallels the rank order of the heteroatomic van der Waals radii (S > N ≥ O) (28), which in turn equals the rank order of relative polarizabilities of these atoms (S > N ≥ O) (45), due to the increase in number of delocalizable electrons with increasing size of the atom.

In conclusion, the present study of heterocyclic *Ah* receptor ligands indicates that the notion (that has emerged from studies on halogenated and aromatic hydrocarbons) of the ligand binding site of *Ah* receptors as a cavity imposing certain (not yet completely mapped) steric restrictions also seems to be plausible for the *Ah* receptor binding of heterocyclic ligands. The generalization that has been derived from studies on halogenated and aromatic hydrocarbons (e.g., earlier QSAR studies recently supported by novel structure-activity approaches and thermodynamic analyses) (Refs. 46 and 47 and references therein), that there is a requirement for hydrophobicity for high affinity ligands for the *Ah* receptor, is not contradicted by our present results of free energy calculations for a pair of compounds. Which other properties (e.g., in terms of charge distribution and polarizability) are shared by members of all three classes of high affinity ligands, i.e., halogenated aromatic hydrocarbons, PAHs (as well as β-naphthoflavone), and heterocyclic ligands, remains to be more firmly established.

Acknowledgments

We thank Dr. S. Wold for provision of the data in Table 2, Dr. P. Kollman for valuable discussions regarding free energy perturbations, and Dr. LeRoy H. Klemm and Dr. P. Kirby for kind submission of samples.

References

1. Burbach, K. M., A. Poland, and C. A. Bradfield. Cloning of the *Ah*-cDNA reveals distinctive ligand-activated transcription factor. *Proc. Natl. Acad. Sci. USA* **89**:8185–8189 (1992).
2. Ema, M., K. Sogawa, N. Watanabe, Y. Chujoh, N. Matsushita, O. Gotoh, Y. Funae, and Y. Fujii-Kuriyama. cDNA cloning and structure of mouse putative Ah receptor. *Biochem. Biophys. Res. Commun.* **184**:246–253 (1992).
3. Reyes, H., S. Reisz-Porszasz, and O. Hankinson. Identification of the Ah receptor nuclear translocator protein (Arnt) as a component of the DNA binding form of the Ah receptor. *Science (Washington D. C.)* **256**:1193–1195 (1992).
4. Poland, A., and J. C. Knutson. 2,3,7,8-Tetrachlorodibenzo-*p*-dioxin and related halgenated hydrocarbons: examination of the mechanism of toxicity. *Annu. Rev. Pharmacol. Toxicol.* **22**:517–554 (1982).
5. Gillner, M., J. Bergman, C. Cambillau, B. Fernström, and J.-Å. Gustafsson. Interactions of indoles with binding sites for 2,3,7,8- tetrachlorodibenzo-*p*-dioxin in rat liver. *Mol. Pharmacol.* **28**:357–363 (1985).
6. Bergman, J. Condensation of indole and formaldehyde in the presence of air and sensitizers: a facile synthesis of indolo[3,2-*b*]carbazole. *Tetrahedron* **26**:3353–3355 (1970).
7. Wattenberg, L. W. Inhibitors of chemical carcinogens, in *Cancer Achievements, Challenges, and Prospects for the 1980s* (J. H. Burchenall and M. F. Oettgen, eds.), Vol 7. Grune & Stratton, New York, 517–539 (1980).
8. Vang, O., B. Jensen, and H. Autrup. Induction of cytochrome P450IA1 in rat colon and liver by indole-3-carbinol and 5,6-benzoflavone. *Carcinogenesis (Lond.)* **11**:1259–1263 (1990).
9. Bradfield, C. A., and L. F. Bjeldanes. Structure-activity relationships of dietary indoles: a proposed mechanism of action as modifiers of xenobiotic metabolism. *J. Toxicol. Environ. Health* **21**:311–323 (1987).
10. Bjeldanes, L. F., J. Y. Kim, K. R. Grose, J. C. Bartholomew, and C. A. Bradfield. Aromatic hydrocarbon responsiveness-receptor agonists generated from indole-3-carbinol *in vitro* and *in vivo*: comparisons with 2,3,7,8-tetrachlorodibenzo-*p*-dioxin. *Proc. Natl. Acad. Sci. USA* **88**(suppl.):9543–9547 (1991).
11. Rannug, A., U. Rannug, H. S. Rozenkranz, L. Winqvist, R. Westerholm, E. Agurell, and A.-K. Grafström. Certain photo-oxidized derivatives of tryptophan bind with very high affinity to the Ah-receptor and are likely to be endogenous signal substances. *J. Biol. Chem.* **262**:15422–15427 (1987).
12. Gillner, M., J. Bergman, C. Cambillau, and J.-Å. Gustafsson. Interactions of rutecarpine alkaloids with specific binding sites for 2,3,7,8-tetrachlorodibenzo-*p*-dioxin in rat liver. *Carcinogenesis (Lond.)* **10**:651–654 (1989).
13. Perdew, G. H., and C. F. Babbs. Production of Ah receptor ligands in rat fecal suspensions containing tryptophan or indole-3-carbinol. *Nutr. Cancer* **16**:209–218 (1991).
14. Johansson, G., M. Gillner, B. Högberg, and J.-Å. Gustafsson. The TCDD receptor in rat intestinal mucosa and its dietary ligands. *Nutr. Cancer* **3**:134–144 (1982).
15. Helferich, W. G., and M. S. Denison. Ultraviolet photoproducts of tryptophan can act as dioxin agonists. *Mol. Pharmacol.* **40**:674–678 (1991).
16. van Gunsteren, W. F., and P. K. Weiner, eds. *Computer Simulations of Biomolecular Systems: Theoretical and Experimental Applications.* Escom-Science, Leiden, The Netherlands (1990).
17. Bash, P. A., U. C. Sing, R. Langridge, and P. A. Kollman. Free energy calculations by computer simulation. *Science (Washington D. C.)* **236**:564–576 (1987).
18. Bergman, J., B. Egestad, and D. Rajapaksa. An X-ray crystal and molecular structure determination of a benzo[1,2-*b*:4,5-*b'*]bisbenzofuran derivative formed by base-induced condensation of ^{3}(^{2}H)-benzofuranone. *Acta Chem. Scand. Ser. B Org. Chem. Biochem.* **33**:405–409 (1979).
19. Hunig, S., and H.-C. Steinmetzer. Kondensierte Stickstoffheterocyclen. *Liebigs Ann. Chem.* 1090–1102 (1976).
20. Robinson, B. The Fischer indolisation of cyclohexane-1,4-dione bisphenylhydrazone. *J. Chem. Soc.* 3097–3099 (1963).
21. Bergman, J., and P. Sand. A new simple procedure for alkylation of nitrogen heterocycles using dialkyl oxalates and alkoxides. *Tetrahedron Lett.* 1957–1961 (1984).
22. Osman, A. M., A. S. Hamman, and A. T. Salah. New diindoloquinones from halogenated *p*-benzoquinones and aromatic amines. *Indian J. Chem. Sect. B Org. Chem. Incl. Med. Chem.* **15**:1118–1120 (1977).
23. Iball, J., and C. H. Morgan. Refinement of the crystal structure of orthorhombic dibenz[*a,h*]anthracene. *J. Chem. Soc. Perkin Trans. II* 1271–1272 (1975).
24. Iball, J., and S. N. Scrimgeour. 20-Methylcholanthrene (a new refinement). *Acta Crystallogr. B Struct. Crystallogr. Cryst. Chem.* **31**:2517–2519 (1975).
25. Sayre, D., and P. H. Friedlander. Crystal structure of 1:2-benz[*a*]anthracene. *Nature (Lond.)* **178**:999–1000 (1956).
26. Iball, J. A refinement of the structure of 9,10-dimethyl-1,2-benz[*a*]anthracene. *Nature (Lond.)* **201**:916–917 (1964).
27. Dideberg, O., L. Dupont, and J. M. Andre. The crystal structure of dibenzofuran. *Acta Crystallogr. B Struct. Crystallogr. Cryst. Chem.* **28**:1002–1007 (1972).
28. Pauling, L. *The Nature of the Chemical Bond*, Ed. 2. Cornell University Press, Ithaca, NY, 224 (1949).
29. Poland, A., W. F. Greenlee, and A. S. Kende. Studies on the mechanism of action of the chlorinated dibenzo-*p*-dioxins and related compounds. *Ann. N. Y. Acad. Sci.* **320**:214–230 (1979).
30. Seydel, J. K., and K.-J. Shaper. *Chemische Struktur und Biologische Aktivitat von Wirkstoffen.* Verlag Chemie, Weinheim (1979).
31. Pullman, A., and B. Pullman. Electronic structure and carcinogenic activity of aromatic molecules. *Adv. Cancer Res.* **3**:117–169 (1955).
32. Knutson, J. C., and A. Poland. Keratinization of mouse teratoma cell line XB produced by 2,3,7,8-tetrachlorodibenzo-*p*-dioxin: an *in vitro* model of toxicity. *Cell* **22**:27–36 (1980).
33. Poland, A., and E. Glover. Stereospecific, high affinity binding of 2,3,7,8-tetrachlorodibenzo-*p*-dioxin by hepatic cytosol: evidence that the binding species is receptor for induction of aryl hydrocarbon hydroxylase. *J. Biol. Chem.* **251**:4936–4946 (1976).
34. Hine, J., and P. K. Mookerjee. The intrinsic hydrophilic character of organic compounds: correlations in terms of structural contributions. *J. Org. Chem.* **40**:292–298 (1975).
35. Johnels, D., M. Gillner, B. Nordén, R. Toftgård, and J.-Å. Gustafsson. Quantitative structure-activity relationship (QSAR) analysis using the partial least square (PLS) method: the binding of polycyclic aromatic hydrocarbons

(PAH) to the rat liver 2,3,7,8-tetrachlorodibenzo-*p*-dioxin in rat liver. *Quant. Structure-Activity Relat.* **8**:83–89 (1989).
36. Maitland, C. G., M. Rigby, E. B. Smith, and W. A. Wakeham. Theoretical calculations of intermolecular forces, in *Intermolecular Forces: Their Origin and Determination*. Clarendon Press, Oxford, UK, 45–95 (1987).
37. Fleischman, S. H., and C. L. Brooks III. Protein-drug interactions: characterization of inhibitor binding in complexes of DHFR with trimethoprim and related derivatives. *Proteins* **7**:52–61 (1990).
38. Grotta, H. M., C. J. Riggle, and A. E. Bearse. Preparation of some condensed ring carbazole derivatives. *J. Org. Chem.* **26**:1509–1511 (1961).
39. Grethe, G., ed. *Isoquinolines. The Chemistry of Heterocyclic Compounds*, Vol. 38, Part 1. Wiley, New York (1981).
40. Keene, B. R. T., and P. Tissington. Phenanthridines. *Adv. Heterocycle Chem.* **13**:315–413 (1971).
41. Jorgensen, W. L., J. M. Briggs, and M. L. Contreras. Relative partitioning coefficients for organic solutes from fluid simulations. *J. Phys. Chem.* **94**:1683–1686 (1990).
42. Politzer, P. Computational approaches to the identification of suspect toxic molecules. *Toxicol. Lett.* **43**:257–276 (1988).
43. Sjöberg, P., J. S. Murray, T. Brinck, P. Evans, and P. J. Politzer. The use of the electrostatic potential at the molecular surface in recognition interactions: dibenzo-*p*-dioxins and related systems. *J. Mol. Graphics* **8**:81–85 (1990).
44. McKinney, J. D., T. Darden, M. A. Lyerly, and L. G. Pedersen. PCB and related compound binding to the Ah receptor(s): theoretical model based on molecular parameters and molecular mechanics. *Quant. Structure-Activity Relat.* **4**:166–172 (1985).
45. Miller, J. K. Additivity methods in molecular polarizabilities. *J. Am. Chem. Soc.* **112**:8533–8542 (1990).
46. Kafafi, S. A., Y. A. Hussein, H. K. Said, and J. M. Hakimi. A new structure-activity model for *Ah* receptor binding: polychlorinated dibenzo-*p*-dioxins and dibenzofurans. *Chem. Res. Toxicol.* **5**:856–862 (1992).
47. Rosengren, R. S., S. S. Safe, and N. J. Bunce. Kinetics of several tritiated polycholorinated dibenzo-*p*-dioxin and dibenzofuran congeners with hepatic cytosolic *Ah* receptor from the Wistar rat. *Chem. Res. Toxicol.* **5**:376–382 (1992).

Send reprint requests to: Jan-Åke Gustafsson, Department of Medical Nutrition, Karolinska Institute, Huddinge University Hospital F60, NOVUM, S-141 86 Huddinge, Sweden.